Supplement of Earth Surf. Dynam., 14, 115–139, 2026
https://doi.org/10.5194/esurf-14-115-2026-supplement

Earth Surface Dynamics
Open Access
EGU

Supplement of

At-a-site and between-site variability of bedload transport, inferred from continuous surrogate monitoring, and comparison to predictive equations

Dieter Rickenmann

Correspondence to: Dieter Rickenmann (dieter.rickenmann@wsl.ch)

Contents of this file

Tables S1 to S5

Figures S1 to S31

Table S1. Exponents m_{tot}, m_{red} and dimensionless reference shear stresses τ^*_{rD50}, $\tau^{*\prime}_{rD50}$ derived from analysis of temporal variation of bedload transport relation for phase-2 transport conditions.

			W*tot analysis		W*red analysis	
SPG site	**year(s)**	**no. time windows**	**m_{tot}**	**τ^*_{rD50}**	**m_{red}**	**$\tau^{*\prime}_{rD50}$**
Albula	*2016*	*5 double-weeks*				
AB_dw			12.62	0.039	8.47	0.025
AB_dw			15.30	0.042	10.47	0.028
AB_dw			14.04	0.042	9.39	0.028
AB_dw			13.75	0.043	9.38	0.029
AB_dw			12.43	0.037	8.05	0.022
		mean	***13.63***	***0.040***	***9.15***	***0.026***
Navisence	*2011*	*9 double-weeks*				
NA_dw			5.03	0.076	2.01	0.010
NA_dw			6.27	0.092	2.64	0.020
NA_dw			5.97	0.099	2.53	0.023
NA_dw			9.70	0.100	4.59	0.029
NA_dw			7.30	0.093	3.28	0.022
NA_dw			6.92	0.101	3.07	0.026
NA_dw			7.61	0.118	3.41	0.039
NA_dw			3.59	0.123	1.26	0.024
NA_dw			7.16	0.080	3.06	0.015
		mean	***6.62***	***0.098***	***2.87***	***0.023***
Avançon	*2019*	*10 double-weeks*				
AV_dw			10.54	0.115	3.94	0.017
AV_dw			5.38	0.103	1.61	0.005
AV_dw			12.03	0.116	4.61	0.018
AV_dw			17.02	0.112	6.87	0.019
AV_dw			10.73	0.115	4.03	0.017
AV_dw			16.10	0.097	6.45	0.013
AV_dw			14.56	0.113	5.76	0.018
AV_dw			14.00	0.115	5.50	0.019
AV_dw			13.34	0.123	5.20	0.022
VN_dw			5.71	0.198	1.76	0.049
		mean	***11.94***	***0.121***	***4.57***	***0.020***

Table S1. Cont'd

			W*tot analysis		W*red analysis	
Erlenbach A	*1986-1999*	*7 sub-periods*				
EB_pid_A			10.98	0.175	5.87	0.028
EB_pid_A			11.33	0.174	6.14	0.028
EB_pid_A			10.58	0.174	5.70	0.028
EB_pid_A			11.18	0.174	6.02	0.028
EB_pid_A			11.70	0.177	6.15	0.029
EB_pid_A			11.03	0.175	5.91	0.028
EB_pid_A			10.06	0.172	5.48	0.027
		mean	***10.98***	***0.174***	***5.90***	***0.028***
Erlenbach B	*2002-2016*	*6 sub-periods*				
EB_pid_B			8.23	0.159	4.82	0.025
EB_pid_B			11.02	0.176	5.87	0.029
EB_pid_B			11.32	0.176	6.02	0.029
EB_pid_B			10.92	0.175	5.82	0.028
EB_pid_B			9.66	0.169	5.36	0.027
EB_pid_B			13.36	0.179	6.82	0.029
		mean	***10.75***	***0.172***	***5.79***	***0.028***
For comparison, data from Schneider et al. (2015a)						
SEA_SS	14 streams	**mean**	**17.86**	**0.099**	**8.47**	**0.036**
SEA_HS	21 streams	**mean**	**7.51**	**0.037**	**5.15**	**0.028**

Table S2. Albula. Mean ratios of calculated to observed bedload masses for period A and for period B, and results of cumulative sum analysis. Table includes begin and end date of yearly observation period, and squared correlation coefficient R^2 for a linear model (LM) fitted to the function CumSum (Q_{bx}) vs. CumSum (Q_{bM}), determined for values ordered according to increasing Q ("incQ") and for τ^*_{D50} => 1.1 τ^*_{rD50} (Q_1.1).

Period (year)	minutes	rt_year	rt_incQ	R^2 for LM	rt within factor 3 from X minutes	rr_year	rr_incQ	R^2 for LM	rr within factor 3 from X minutes	Qmax (m3/s)	Qmax / Q_1.1
13.05. – 10.09.2016	78761	0.570	0.614	0.969	33000	0.442	0.453	0.978	25000	92.02	4.30
18.05. – 10.08.2017	24668	0.108	0.294	0.962	16000	0.132	0.255	0.998	9000	29.20	1.36
23.04. – 31.10.2018	36888	0.253	0.251	0.989	3200	0.224	0.210	0.991	2100	44.22	2.07
02.06. – 31.10.2019	44633	0.907	0.796	0.991	5700	0.670	0.597	0.993	5600	108.30	5.06
11.05. – 10.10.2020	39952	0.230	0.336	0.920	29000	0.185	0.264	0.931	29000	54.48	2.55
10.05. – 20.06.2021	27076	0.162	0.218	0.926	19000	0.134	0.177	0.936	18000	40.56	1.90
01.01. – 31.12.2022	22171	0.035	0.260	0.999	NA	0.067	0.243	0.997	NA	24.39	1.14
13.05. – 25.10.2023	43890	0.584	0.910	0.992	37000	0.428	0.663	0.993	37000	84.80	3.96
Mean		0.356	0.460		20414	0.285	0.358		17957		

Table S3. Navisence. Mean ratios of calculated to observed bedload masses for period A and for period B, and results of cumulative sum analysis. Table includes begin and end date of yearly observation period, and squared correlation coefficient R^2 for a linear model (LM) fitted to the function CumSum (Q_{bx}) vs. CumSum (Q_{bM}), determined for values ordered according to increasing Q ("incQ") and for τ^*_{D50} => 1.1 τ^*_{rD50} (Q_1.1).

Period (year)	minutes	rt_year	rt_incQ	R^2 for LM	rt within factor 3 from X minutes	rr_year	rr_incQ	R^2 for LM	rr within factor 3 from X minutes	Qmax (m3/s)	Qmax / Q_1.1
18.05. – 30.09.2011	186439	0.066	1.575	0.801	NA	0.437	5.724	0.861	NA	30.69	1.65
01.05. – 30.09.2012	220319	0.049	0.590	0.876	NA	0.630	2.949	0.932	NA	23.10	1.24
01.05. – 07.08.2013	142384	0.461	0.704	0.988	(73000)	2.991	2.653	0.997	73000	33.23	1.79
18.07. – 30.09.2019	66436	0.490	1.423	0.915	32000	3.055	5.430	0.956	25000	34.44	1.85
02.05. – 30.09.2020	117214	0.384	1.914	0.995	NA	3.002	8.468	0.999	57000	27.41	1.47
10.05. – 30.09.2021	105612	0.879	3.067	0.983	(24000)	7.043	14.500	0.996	19000	26.92	1.45
Mean		0.388	1.546		32000	2.860	6.621		43500		

Table S4. Avançon. Mean ratios of calculated to observed bedload masses for period A and for period B, and results of cumulative sum analysis. Table includes begin and end date of yearly observation period, and squared correlation coefficient R^2 for a linear model (LM) fitted to the function CumSum (Q_{bx}) vs. CumSum (Q_{bM}), determined for values ordered according to increasing Q ("incQ") and for τ^*_{rD50} => 1.1 τ^*_{rD50} (Q_1.1).

Period (year)	minutes	rt_year	rt_incQ	R^2 for LM	rt within factor 3 from X minutes	rr_year	rr_incQ	R^2 for LM	rr within factor 3 from X minutes	Qmax (m3/s)	Qmax / Q_1.1
16.04. – 29.10.2018	139106	5.663	8.135	0.996	28000	0.882	0.973	0.979	30000	6.88	4.74
17.04. – 31.10.2019	146560	5.221	6.287	0.830	23000	1.460	1.459	0.704	25000	6.14	4.23
14.04. – 30.08.2020	90302	3.593	6.588	0.990	16000	0.386	0.577	0.937	20000	4.66	3.21
25.04. – 26.09.2021	23608	5.875	7.389	0.979	4700	0.588	0.700	0.906	5000	2.79	1.92
10.05. – 31.10.2022	37562	4.633	4.793	0.292	6700	1.954	1.519	0.694	16000	6.90	4.76
18.04. – 30.10.2023	95707	11.346	14.420	0.985	91	2.820	2.436	0.853	216	6.86	4.73
Mean		6.055	7.935		13082	1.349	1.277		16036		

Table S5. Erlenbach. Mean ratios of calculated to observed bedload masses for period A and for period B, and results of cumulative sum analysis. Table includes begin and end date of yearly observation period, and squared correlation coefficient R^2 for a linear model (LM) fitted to the function CumSum (Q_{bx}) vs. CumSum (Q_{bM}), determined for values ordered according to increasing Q ("incQ") and for τ^*_{rD50} => 1.1 τ^*_{rD50} (Q_1.1).

Period (year)	minutes	rt_year	rt_incQ	R^2 for LM	rt within factor 3 from X minutes	rr_year	rr_incQ	R^2 for LM	rr within factor 3 from X minutes	Qmax (m3/s)	Qmax / Q_1.1
20.10.1986 - 30.09.1999	37930	0.840	0.994	0.969	0	0.248	0.163	0.916	3100	9.80	14.83
16.11.2002 - 26.10.2016	33917	0.817	0.940	0.980	3800	0.343	0.218	0.870	4700	15.60	23.60
Mean		0.829	0.967		1900	0.295	0.191		3900		

Q_b vs. Q plots for the Albula

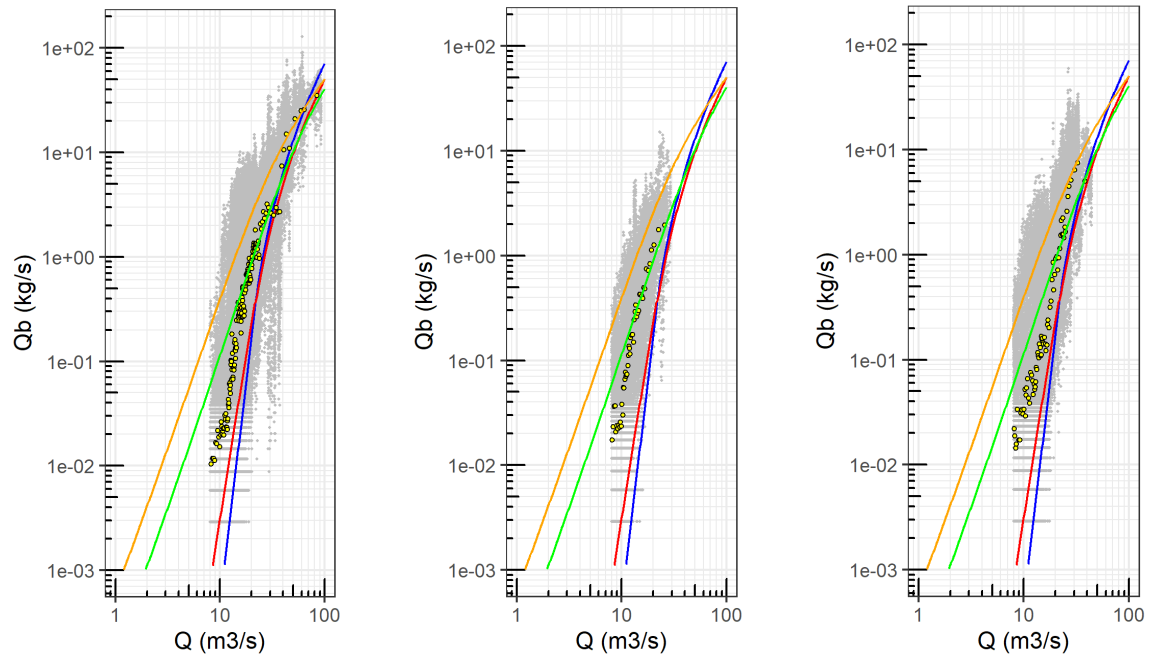

Figure S1. Albula, Q_b vs. Q plots with 4 bedload equations, for (a) 2016, (b) 2017, (c) 2018. The legend is the same as in Figure 3 of the paper. The binned geometric mean values of Q_b for binned Q classes were determined by setting zero Q_b values to Q_b = 1e-4 kg/s, to match the $Q_{bM\ binned}$ values for the Albula 2016 in Figure 3.

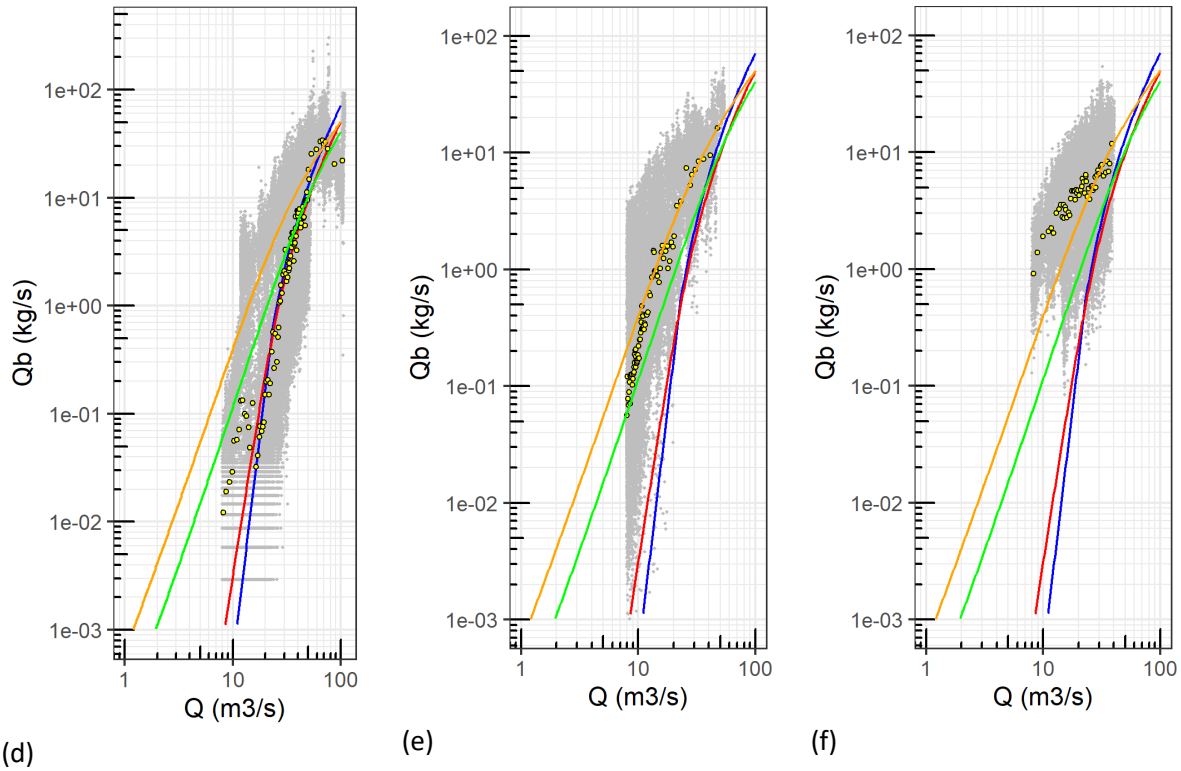

Figure S2. Albula, Q_b vs. Q plots with 4 bedload equations, for (d) 2019, (e) 2020, (f) 2021. The legend is the same as in Figure 3 of the paper. The binned geometric mean values of Q_b for binned Q classes were determined by setting zero Q_b values to Q_b = 1e-4 kg/s, to match the $Q_{bM\ binned}$ values for the Albula 2016 in Figure 3.

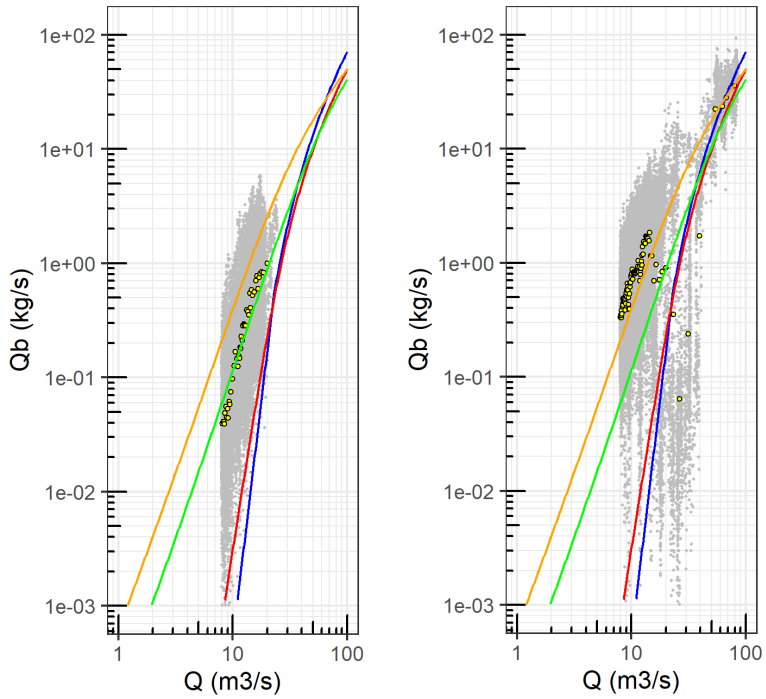

(g) (h)

Figure S3. Albula, Q_b vs. Q plots with 4 bedload equations, (g) 2022, (h) 2023. The legend is the same as in Figure 3 of the paper. The binned geometric mean values of Q_b for binned Q classes were determined by setting zero Q_b values to Q_b = 1e-4 kg/s, to match the $Q_{bM\ binned}$ values for the Albula 2016 in Figure 3.

CumSum analysis for the Albula

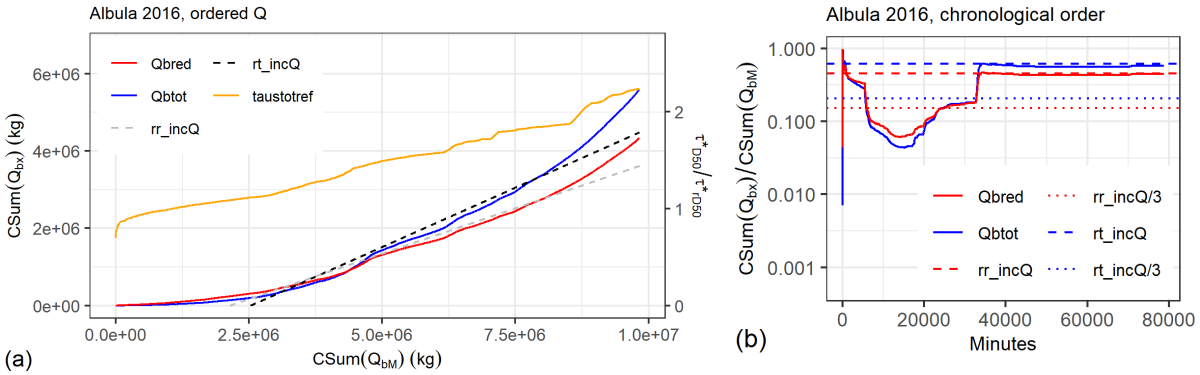

Figure S4. Albula, summer 2016. (a) Application of a liner model (gray and black dashed lines) for the cumulative sum of calculated (SumQbx) vs. measured (SumQbM) bedload masses; values are ordered according to increasing discharge Q. (b) Ratio of cumulative sum of calculated (CSum(Qbx)) to cumulative sum of observed (CSum(QbM)) bedload masses vs. time (in minutes); values are in chronological order.

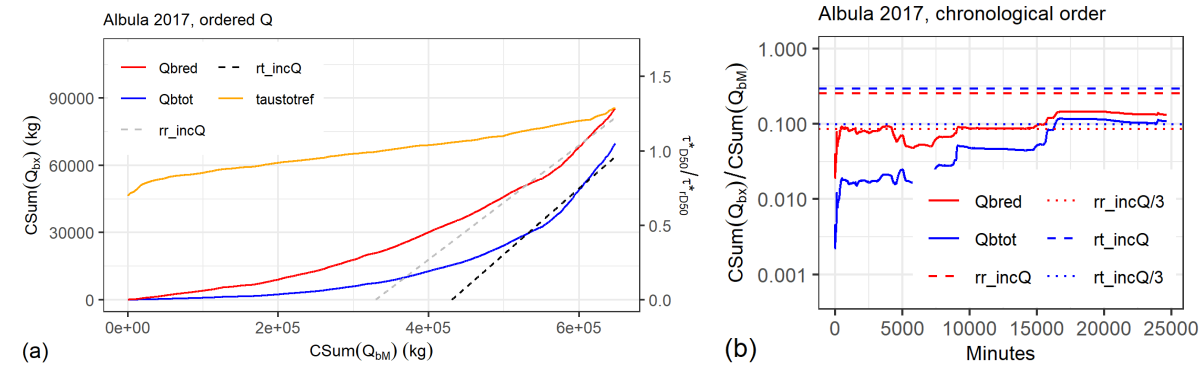

Figure S5. Albula, summer 2017. (a) Application of a liner model (gray and black dashed lines) for the cumulative sum of calculated (SumQbx) vs. measured (SumQbM) bedload masses; values are ordered according to increasing discharge Q. (b) Ratio of cumulative sum of calculated (CSum(Qbx)) to cumulative sum of observed (CSum(QbM)) bedload masses vs. time (in minutes); values are in chronological order.

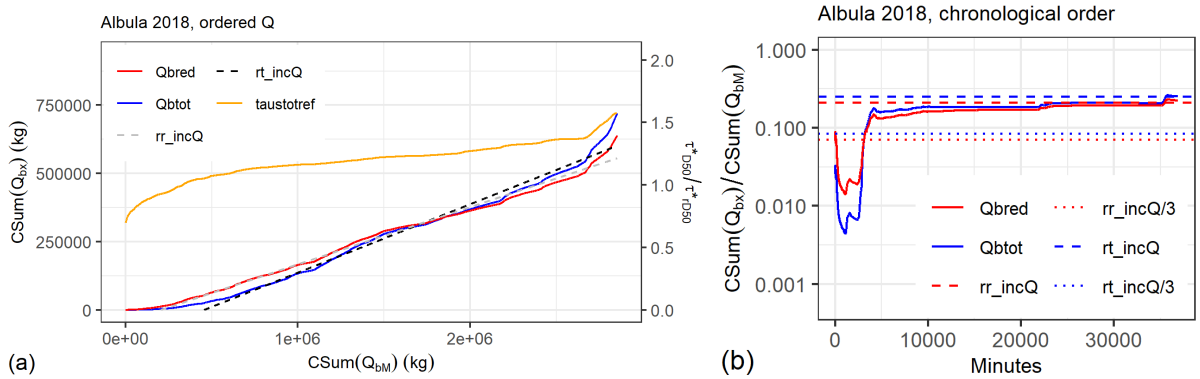

Figure S6. Albula, summer 2018. (a) Application of a liner model (gray and black dashed lines) for the cumulative sum of calculated (SumQbx) vs. measured (SumQbM) bedload masses; values are ordered according to increasing discharge Q. (b) Ratio of cumulative sum of calculated (CSum(Qbx)) to cumulative sum of observed (CSum(QbM)) bedload masses vs. time (in minutes); values are in chronological order.

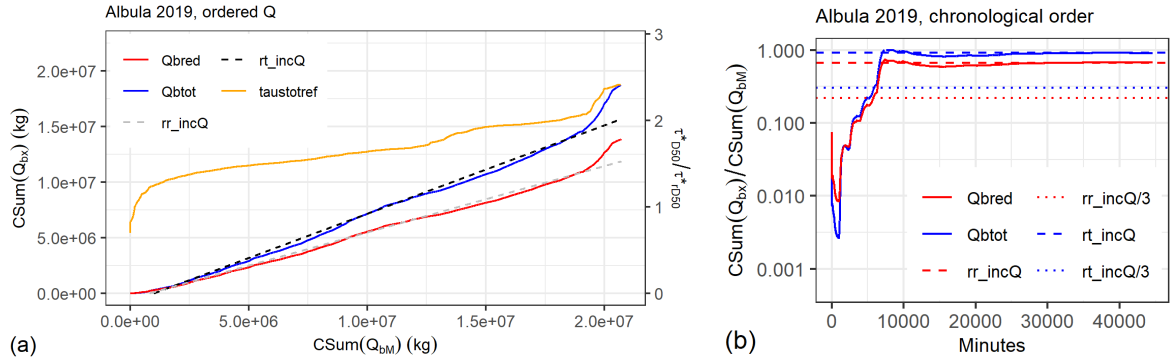

Figure S7. Albula, summer 2019. (a) Application of a liner model (gray and black dashed lines) for the cumulative sum of calculated (SumQbx) vs. measured (SumQbM) bedload masses; values are ordered according to increasing discharge Q. (b) Ratio of cumulative sum of calculated (CSum(Qbx)) to cumulative sum of observed (CSum(QbM)) bedload masses vs. time (in minutes); values are in chronological order.

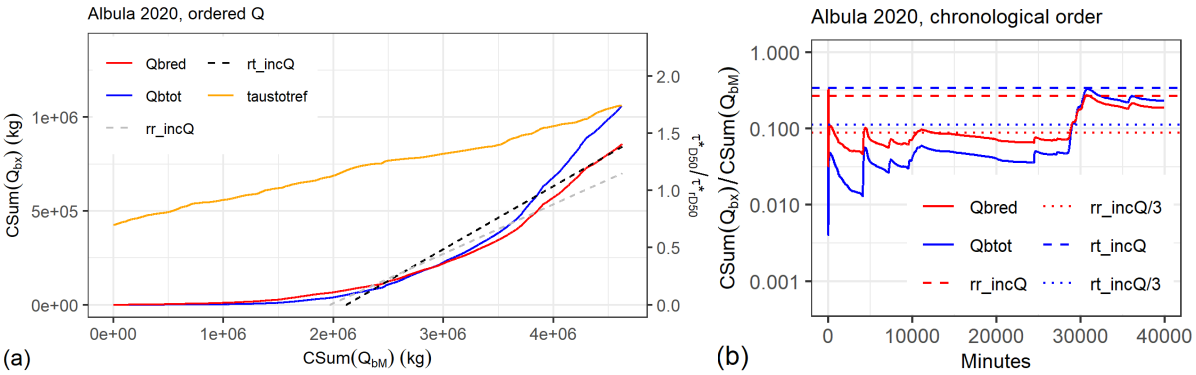

Figure S8. Albula, summer 2020. (a) Application of a liner model (gray and black dashed lines) for the cumulative sum of calculated (SumQbx) vs. measured (SumQbM) bedload masses; values are ordered according to increasing discharge Q. (b) Ratio of cumulative sum of calculated (CSum(Qbx)) to cumulative sum of observed (CSum(QbM)) bedload masses vs. time (in minutes); values are in chronological order.

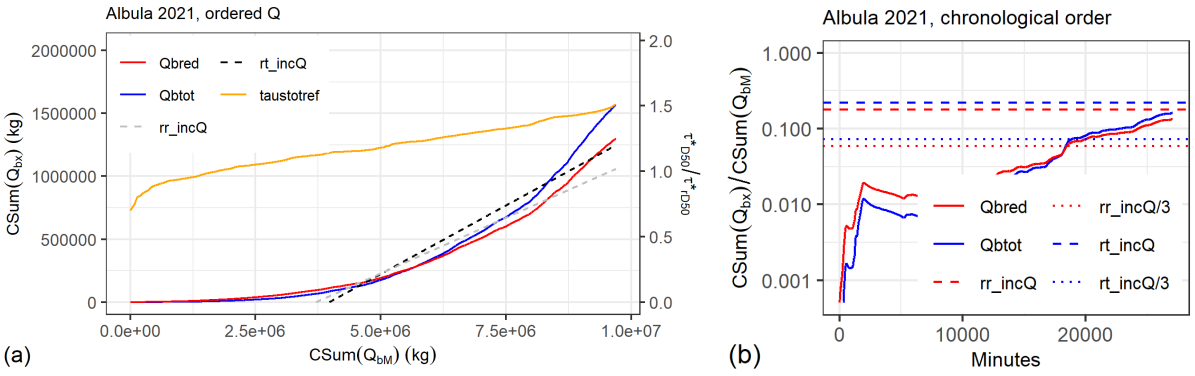

Figure S9. Albula, summer 2021. (a) Application of a liner model (gray and black dashed lines) for the cumulative sum of calculated (SumQbx) vs. measured (SumQbM) bedload masses; values are ordered according to increasing discharge Q. (b) Ratio of cumulative sum of calculated (CSum(Qbx)) to cumulative sum of observed (CSum(QbM)) bedload masses vs. time (in minutes); values are in chronological order.

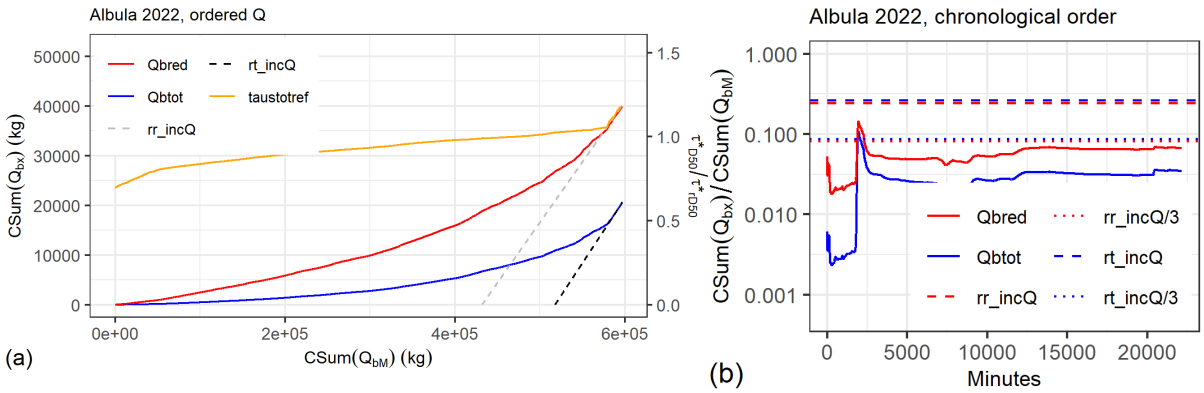

Figure S10. Albula, summer 2022. (a) Application of a liner model (gray and black dashed lines) for the cumulative sum of calculated (SumQbx) vs. measured (SumQbM) bedload masses; values are ordered according to increasing discharge Q. (b) Ratio of cumulative sum of calculated (CSum(Qbx)) to cumulative sum of observed (CSum(QbM)) bedload masses vs. time (in minutes); values are in chronological order.

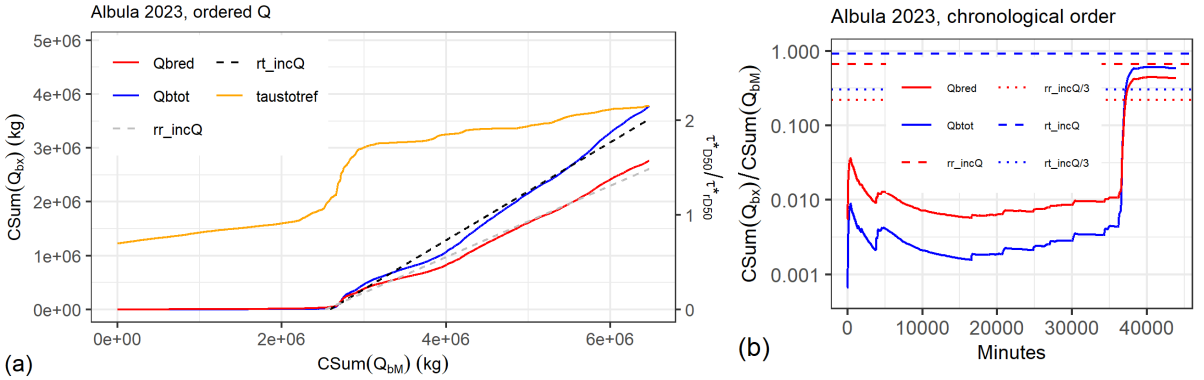

Figure S11. Albula, summer 2023. (a) Application of a liner model (gray and black dashed lines) for the cumulative sum of calculated (SumQbx) vs. measured (SumQbM) bedload masses; values are ordered according to increasing discharge Q. (b) Ratio of cumulative sum of calculated (CSum(Qbx)) to cumulative sum of observed (CSum(QbM)) bedload masses vs. time (in minutes); values are in chronological order.

Q_b vs. Q plots for the Navisence

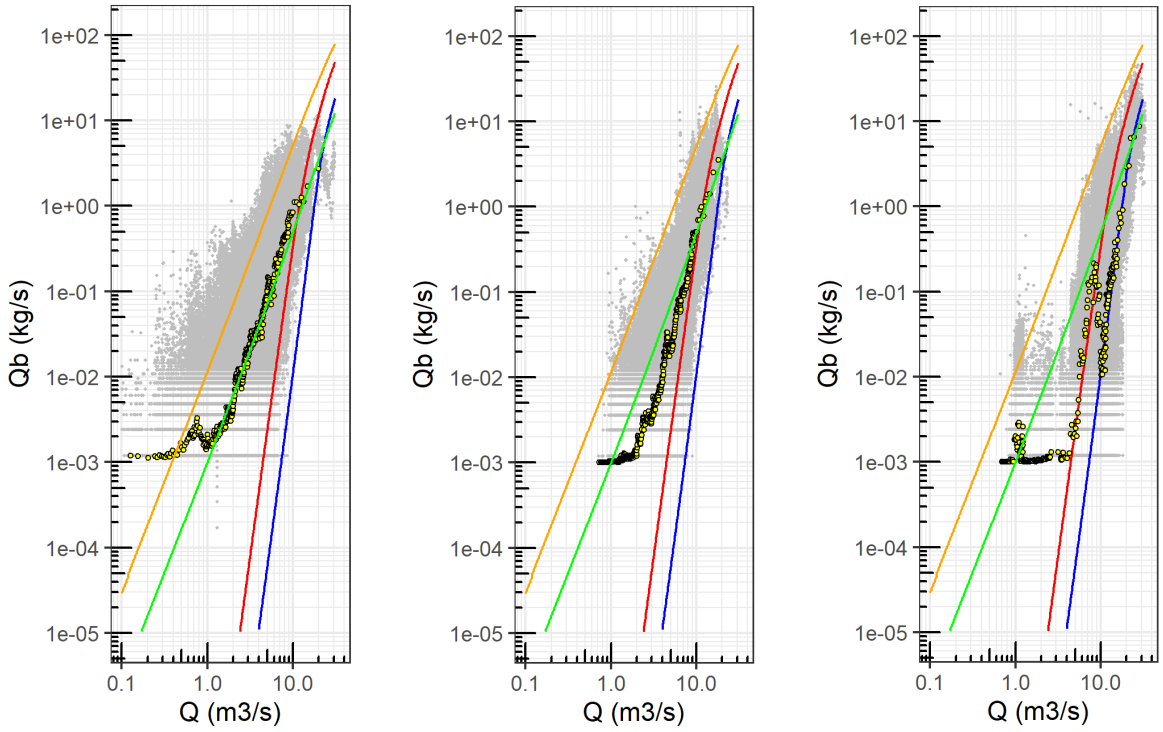

Figure S12. Navisence, Q_b vs. Q plots with 4 bedload equations, for (a) 2011, (b) 2012, (c) 2013. The legend is the same as in Figure 3 of the paper. The binned geometric mean values of Q_b for binned Q classes were determined by setting zero Q_b values to Q_b = 1e-3 kg/s, to match the $Q_{bM\ binned}$ values for the Navisence 2011 in Figure 3.

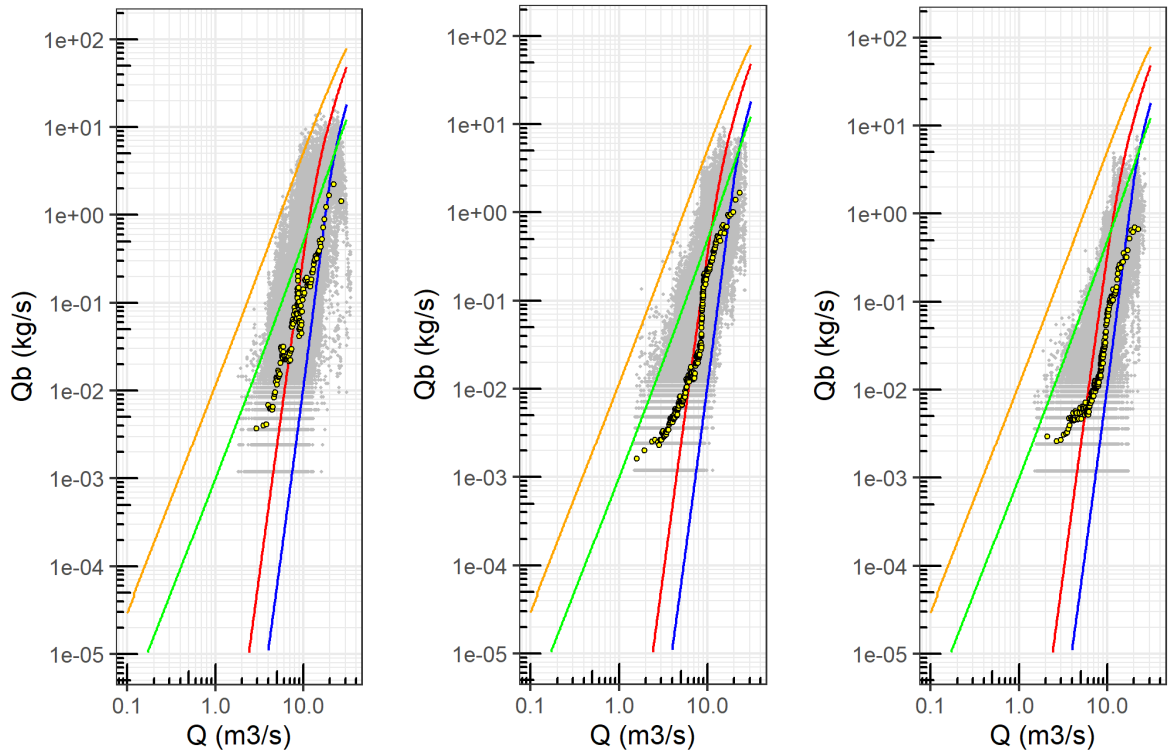

(d) (e) (f)

Figure S13. Navisence, Q_b vs. Q plots with 4 bedload equations, for (d) 2019, (e) 2020, (f) 2021. The legend is the same as in Figure 3 of the paper. The binned geometric mean values of Q_b for binned Q classes were determined by setting zero Q_b values to Q_b = 1e-3 kg/s, to match the $Q_{bM\ binned}$ values for the Navisence 2011 in Figure 3.

CumSum analysis for the Navisence

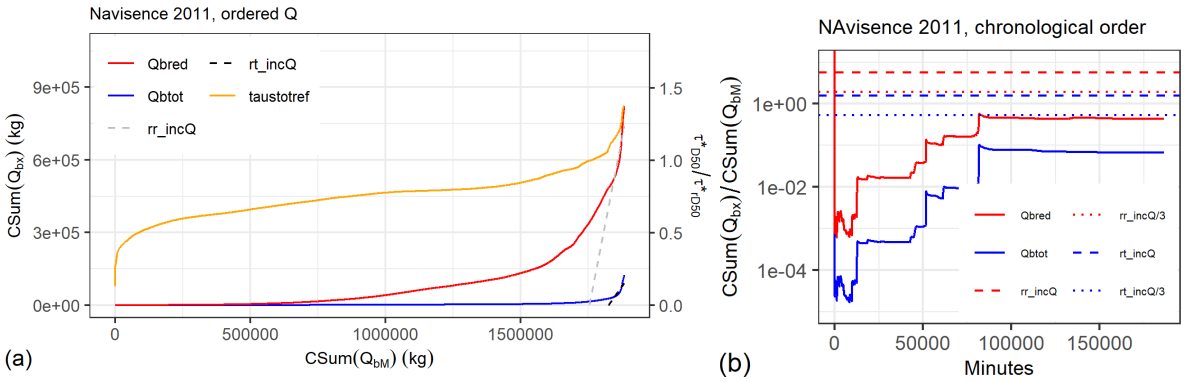

Figure S14. Navisence, summer 2011. (a) Application of a liner model (gray and black dashed lines) for the cumulative sum of calculated (SumQbx) vs. measured (SumQbM) bedload masses; values are ordered according to increasing discharge Q. (b) Ratio of cumulative sum of calculated (CSum(Qbx)) to cumulative sum of observed (CSum(QbM)) bedload masses vs. time (in minutes); values are in chronological order.

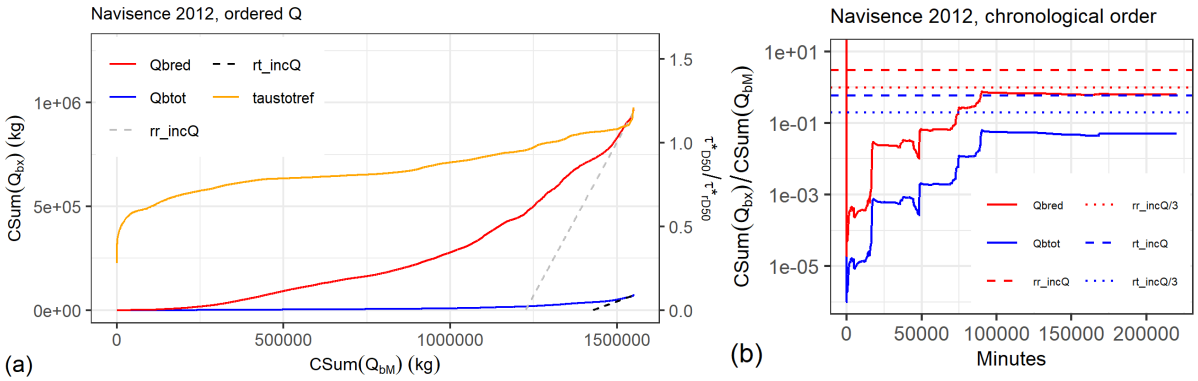

Figure S15. Navisence, summer 2012. (a) Application of a liner model (gray and black dashed lines) for the cumulative sum of calculated (SumQbx) vs. measured (SumQbM) bedload masses; values are ordered according to increasing discharge Q. (b) Ratio of cumulative sum of calculated (CSum(Qbx)) to cumulative sum of observed (CSum(QbM)) bedload masses vs. time (in minutes); values are in chronological order.

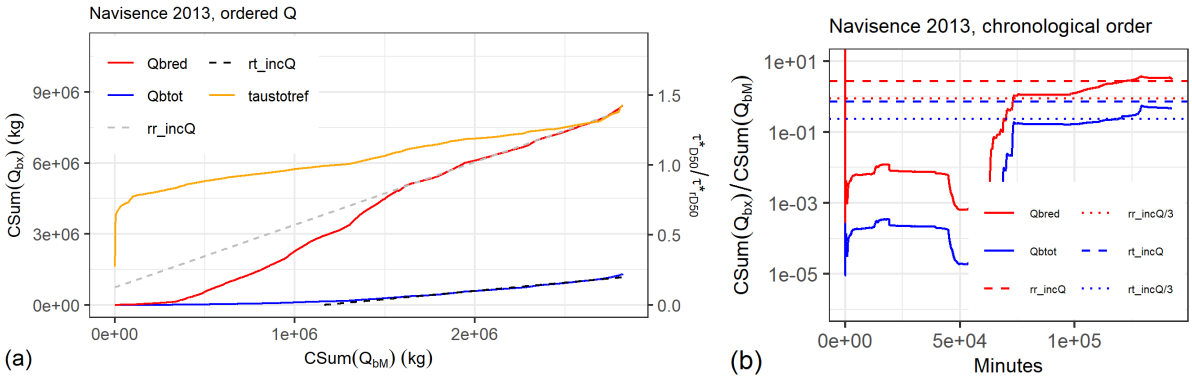

Figure S16. Navisence, summer 2013. (a) Application of a liner model (gray and black dashed lines) for the cumulative sum of calculated (SumQbx) vs. measured (SumQbM) bedload masses; values are ordered according to increasing discharge Q. (b) Ratio of cumulative sum of calculated (CSum(Qbx)) to cumulative sum of observed (CSum(QbM)) bedload masses vs. time (in minutes); values are in chronological order.

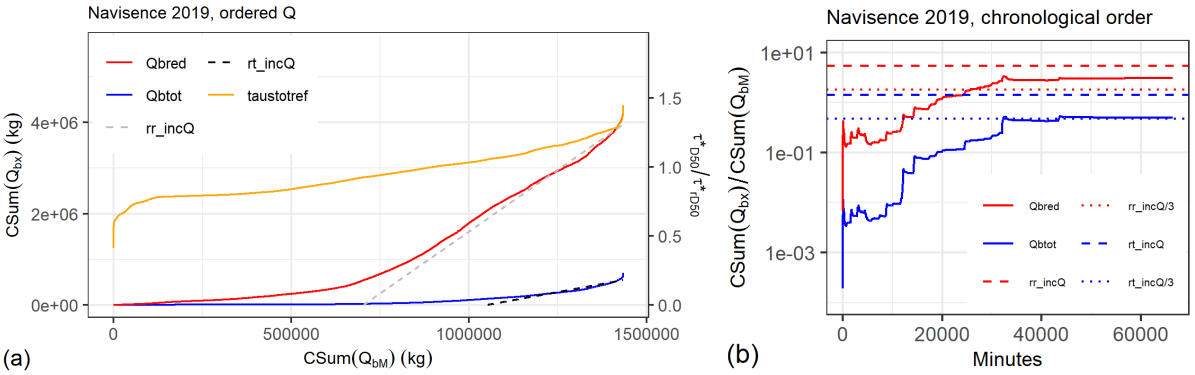

Figure S17. Navisence, summer 2019. (a) Application of a liner model (gray and black dashed lines) for the cumulative sum of calculated (SumQbx) vs. measured (SumQbM) bedload masses; values are ordered according to increasing discharge Q. (b) Ratio of cumulative sum of calculated (CSum(Qbx)) to cumulative sum of observed (CSum(QbM)) bedload masses vs. time (in minutes); values are in chronological order.

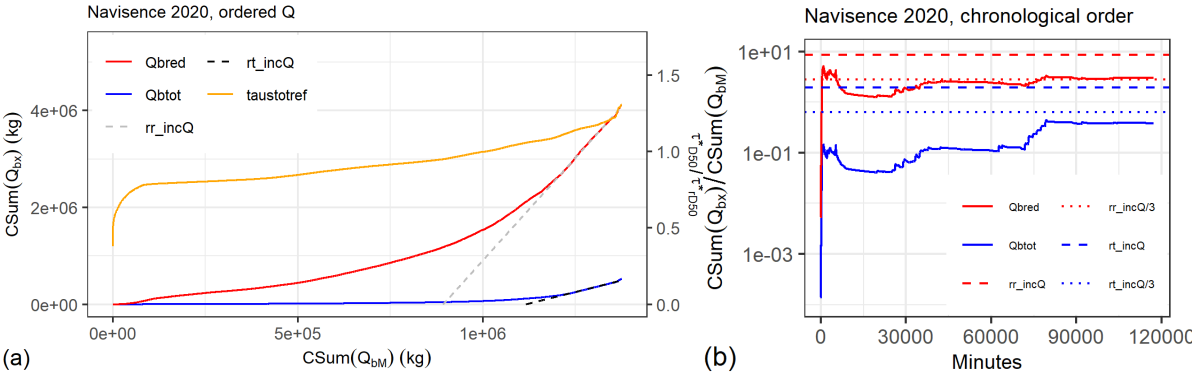

Figure S18. Navisence, summer 2020. (a) Application of a liner model (gray and black dashed lines) for the cumulative sum of calculated (SumQbx) vs. measured (SumQbM) bedload masses; values are ordered according to increasing discharge Q. (b) Ratio of cumulative sum of calculated (CSum(Qbx)) to cumulative sum of observed (CSum(QbM)) bedload masses vs. time (in minutes); values are in chronological order.

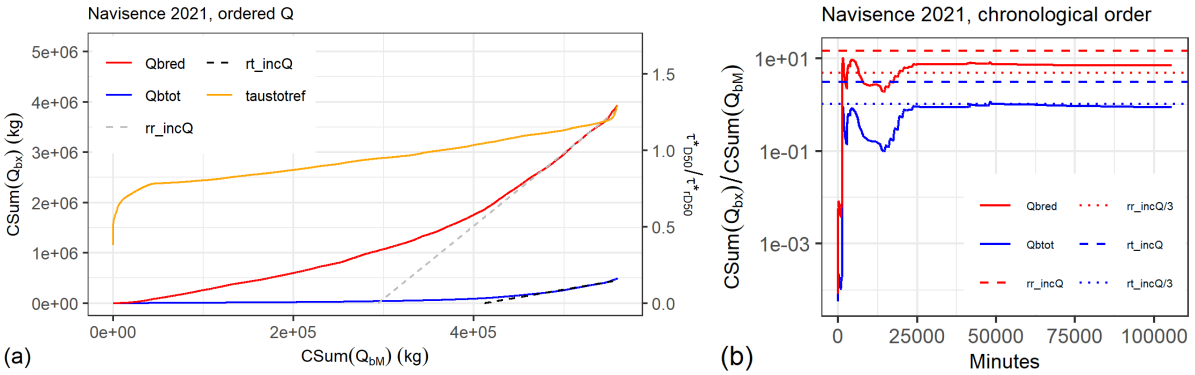

Figure S19. Navisence, summer 2021. (a) Application of a liner model (gray and black dashed lines) for the cumulative sum of calculated (SumQbx) vs. measured (SumQbM) bedload masses; values are ordered according to increasing discharge Q. (b) Ratio of cumulative sum of calculated (CSum(Qbx)) to cumulative sum of observed (CSum(QbM)) bedload masses vs. time (in minutes); values are in chronological order.

Q_b vs. Q plots for the Avançon de Nant

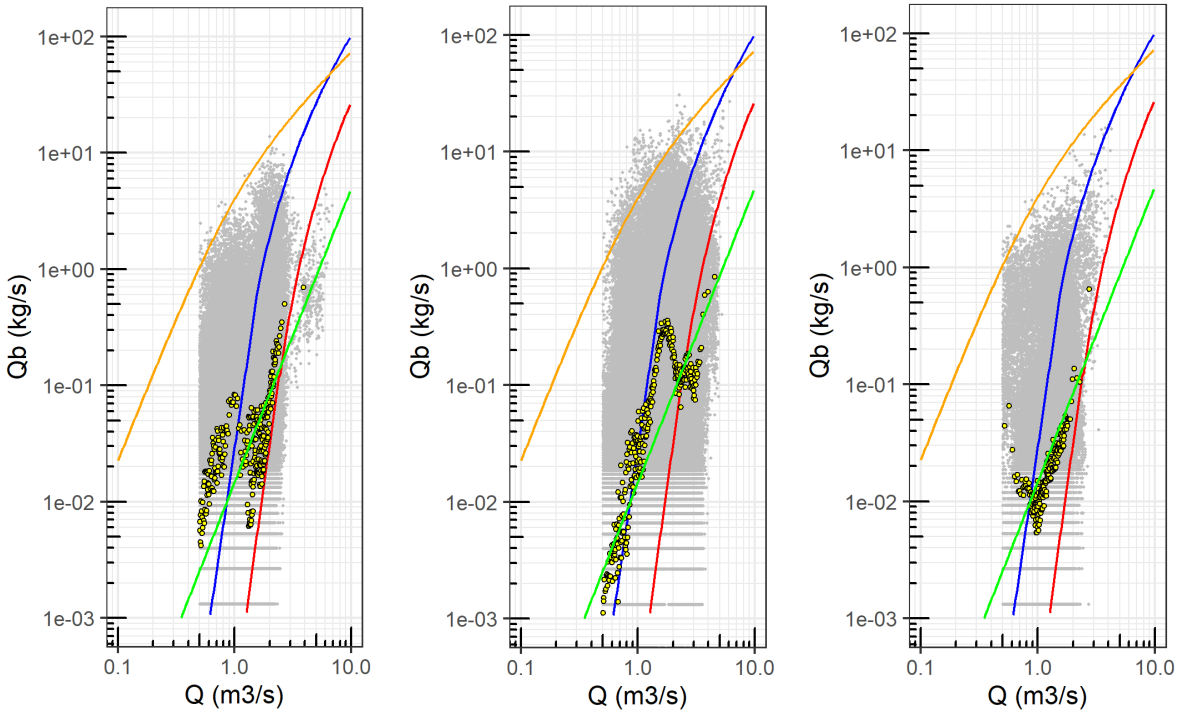

Figure S20. Avançon, Q_b vs. Q plots with 4 bedload equations, for (a) 2018, (b) 2019, (c) 2020. The legend is the same as in Figure 3 of the paper.The binned geometric mean values of Q_b for binned Q classes were determined by setting zero Q_b values to Q_b = 1e-5 kg/s, to match the $Q_{bM\ binned}$ values for the Avancon 2019 in Figure 3.

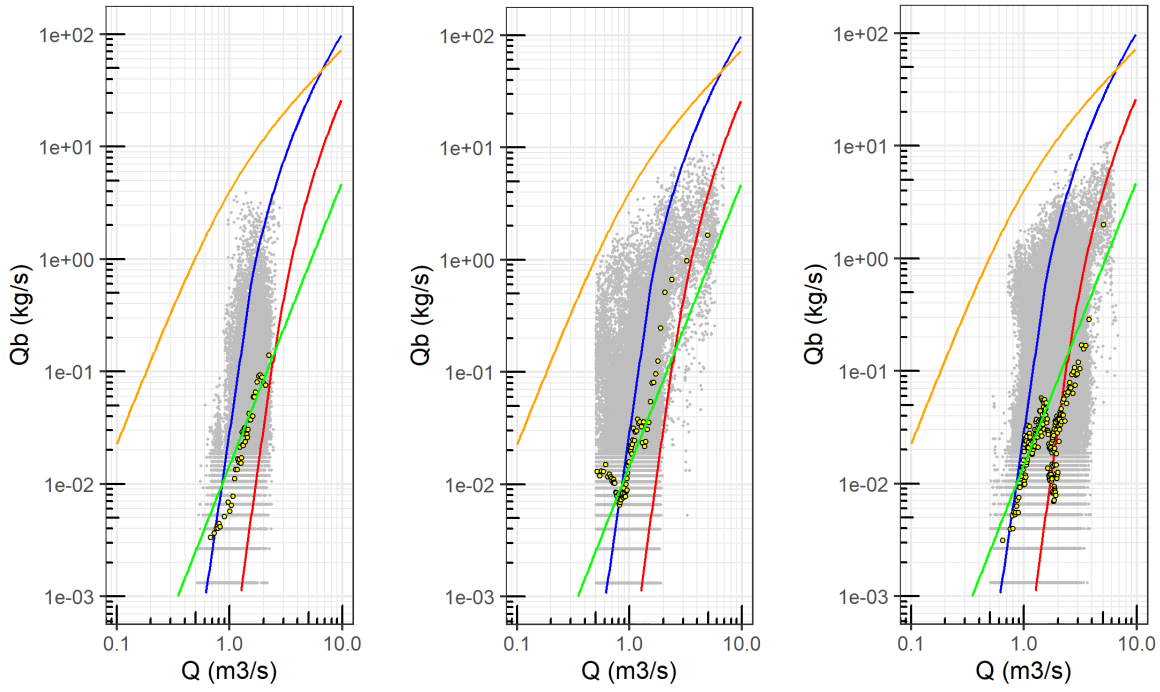

(d) (e) (f)

Figure S21. Avançon, Q_b vs. Q plots with 4 bedload equations, (d) 2021, (e) 2022, (f) 2023. The legend is the same as in Figure 3 of the paper.The binned geometric mean values of Q_b for binned Q classes were determined by setting zero Q_b values to Q_b = 1e-5 kg/s, to match the $Q_{bM\ binned}$ values for the Avancon 2019 in Figure 3.

CumSum analysis for the Avançon de Nant

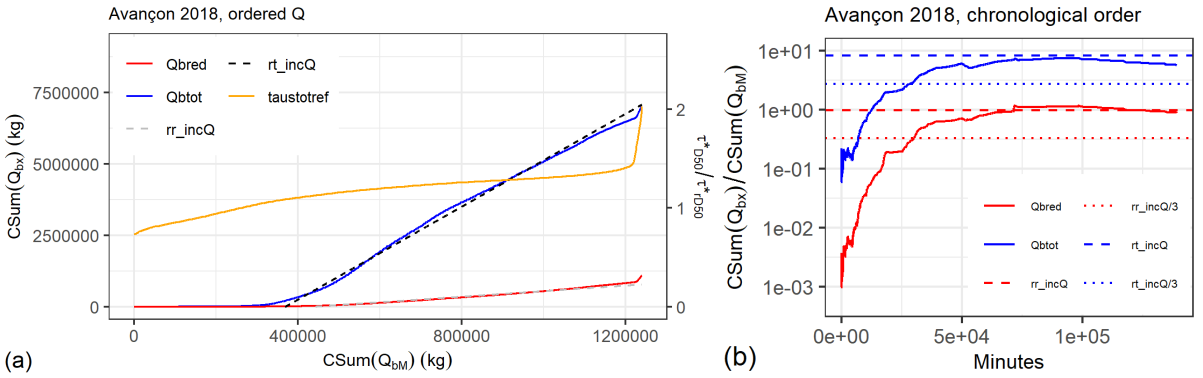

Figure S22. Avançon, summer 2018. (a) Application of a liner model (gray and black dashed lines) for the cumulative sum of calculated (SumQbx) vs. measured (SumQbM) bedload masses; values are ordered according to increasing discharge Q. (b) Ratio of cumulative sum of calculated (CSum(Qbx)) to cumulative sum of observed (CSum(QbM)) bedload masses vs. time (in minutes); values are in chronological order.

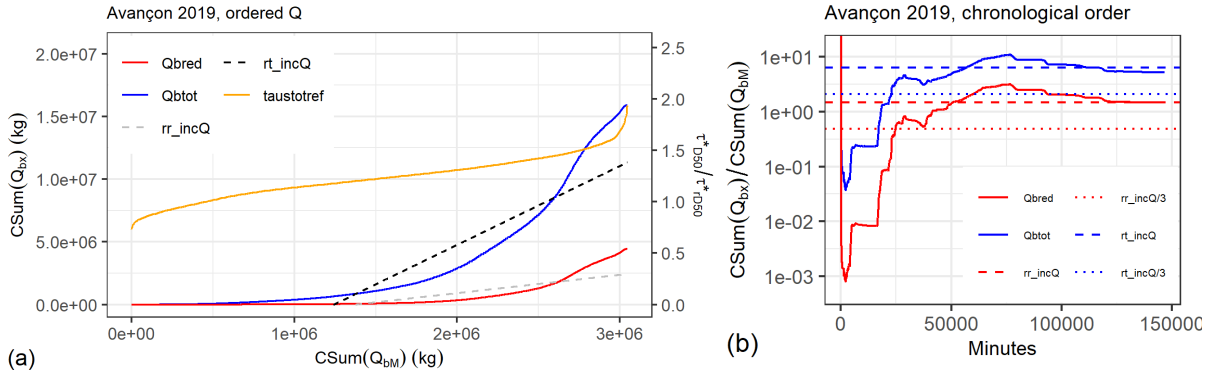

Figure S23. Avançon, summer 2019. (a) Application of a liner model (gray and black dashed lines) for the cumulative sum of calculated (SumQbx) vs. measured (SumQbM) bedload masses; values are ordered according to increasing discharge Q. (b) Ratio of cumulative sum of calculated (CSum(Qbx)) to cumulative sum of observed (CSum(QbM)) bedload masses vs. time (in minutes); values are in chronological order.

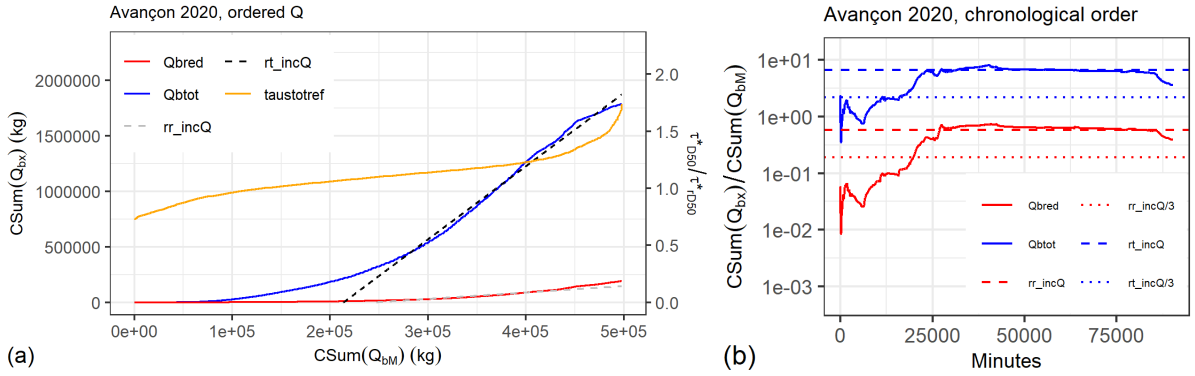

Figure S24. Avançon, summer 2020. (a) Application of a liner model (gray and black dashed lines) for the cumulative sum of calculated (SumQbx) vs. measured (SumQbM) bedload masses; values are ordered according to increasing discharge Q. (b) Ratio of cumulative sum of calculated (CSum(Qbx)) to cumulative sum of observed (CSum(QbM)) bedload masses vs. time (in minutes); values are in chronological order.

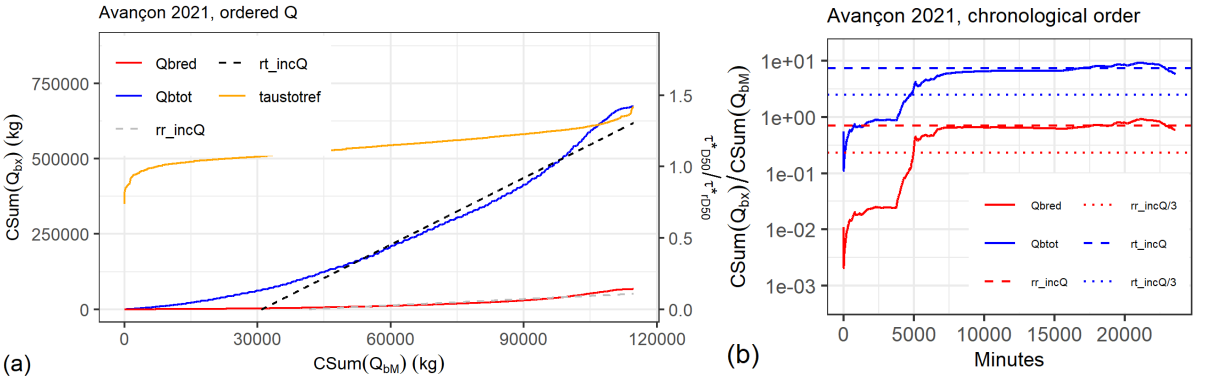

Figure S25. Avançon, summer 2021. (a) Application of a liner model (gray and black dashed lines) for the cumulative sum of calculated (SumQbx) vs. measured (SumQbM) bedload masses; values are ordered according to increasing discharge Q. (b) Ratio of cumulative sum of calculated (CSum(Qbx)) to cumulative sum of observed (CSum(QbM)) bedload masses vs. time (in minutes); values are in chronological order.

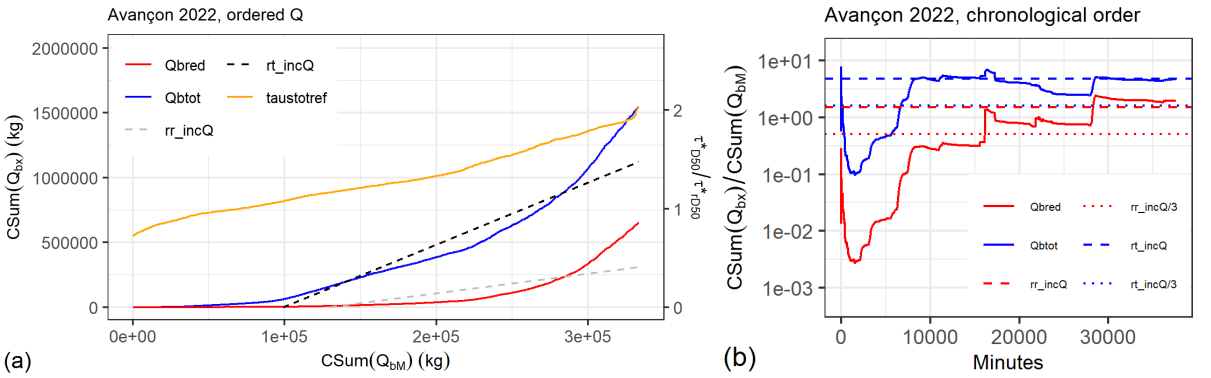

Figure S26. Avançon, summer 2022. (a) Application of a liner model (gray and black dashed lines) for the cumulative sum of calculated (SumQbx) vs. measured (SumQbM) bedload masses; values are ordered according to increasing discharge Q. (b) Ratio of cumulative sum of calculated (CSum(Qbx)) to cumulative sum of observed (CSum(QbM)) bedload masses vs. time (in minutes); values are in chronological order.

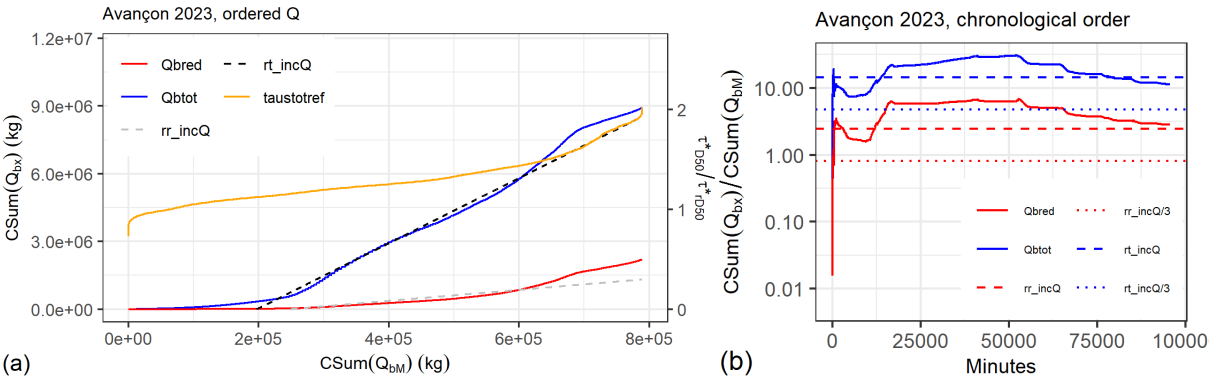

Figure S27. Avançon, summer 2023. (a) Application of a liner model (gray and black dashed lines) for the cumulative sum of calculated (SumQbx) vs. measured (SumQbM) bedload masses; values are ordered according to increasing discharge Q. (b) Ratio of cumulative sum of calculated (CSum(Qbx)) to cumulative sum of observed (CSum(QbM)) bedload masses vs. time (in minutes); values are in chronological order.

Q_b vs. Q plots for the Erlenbach

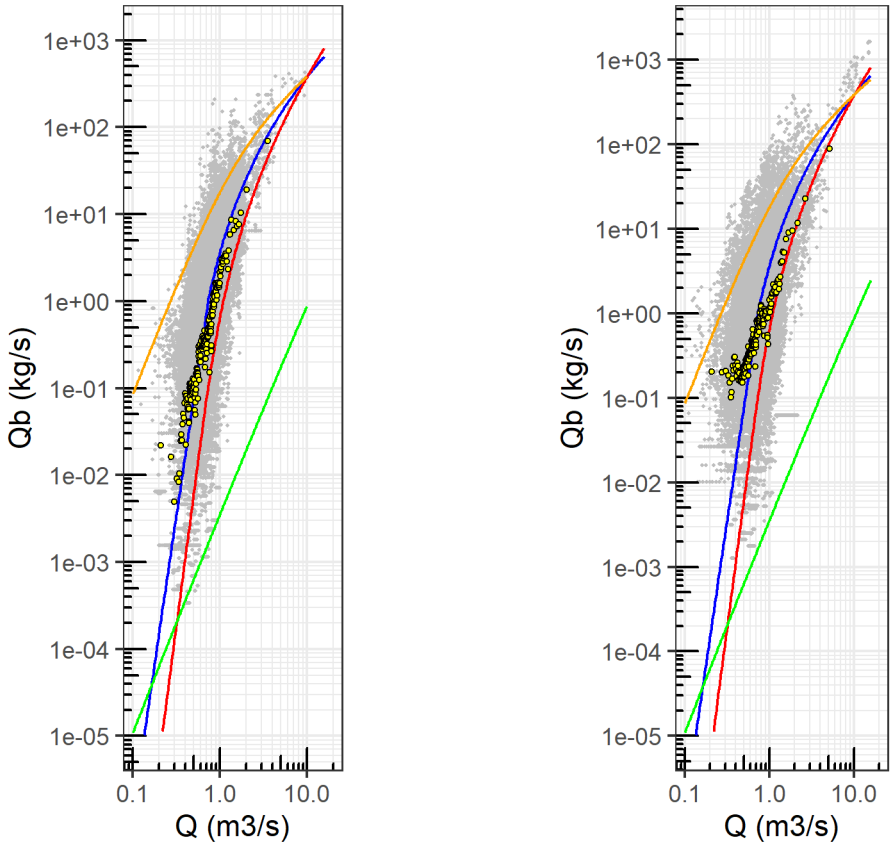

(a) (b)

Figure S28. Erlenbach, Q_b vs. Q plots with 4 bedload equations, for (a) 1986-1999 (period A), and (b) 2012-2016 (period B). The legend is the same as in Figure 3 of the paper.

CumSum analysis for the Erlenbach

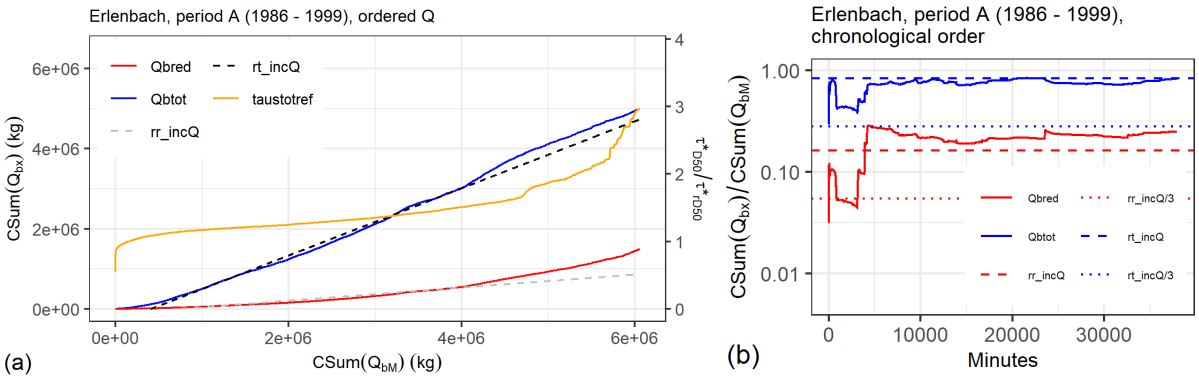

Figure S29. Erlenbach, period A. (a) Application of a liner model (gray and black dashed lines) for the cumulative sum of calculated (SumQbx) vs. measured (SumQbM) bedload masses; values are ordered according to increasing discharge Q. (b) Ratio of cumulative sum of calculated (CSum(Qbx)) to cumulative sum of observed (CSum(QbM)) bedload masses vs. time (in minutes); values are in chronological order.

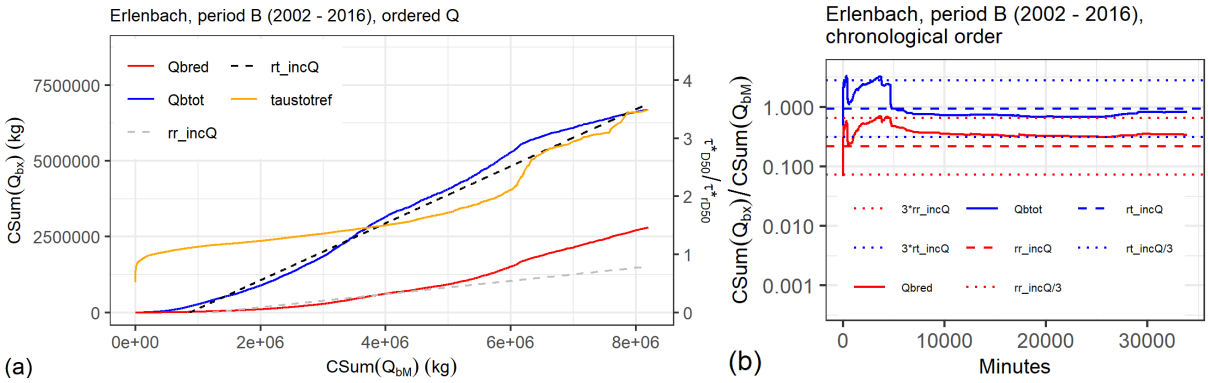

Figure S30. Erlenbach, period B. (a) Application of a liner model (gray and black dashed lines) for the cumulative sum of calculated (SumQbx) vs. measured (SumQbM) bedload masses; values are ordered according to increasing discharge Q. (b) Ratio of cumulative sum of calculated (CSum(Qbx)) to cumulative sum of observed (CSum(QbM)) bedload masses vs. time (in minutes); values are in chronological order.

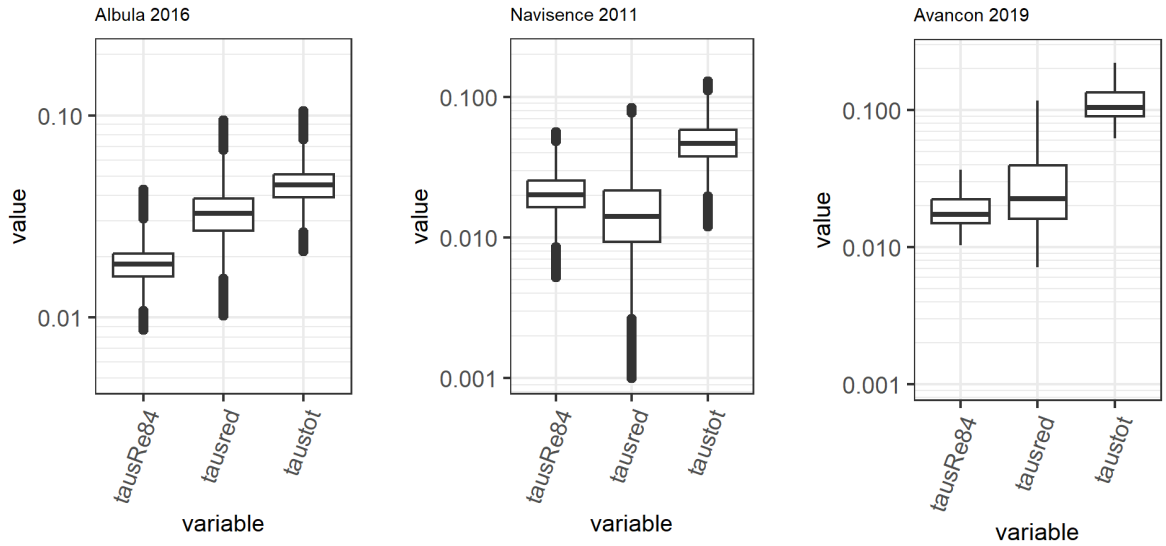

(a) (b) (c)

Figure S31. Boxplots of tausRe84 (τ^*_{Re84}), tausred ($\tau^{*'}_{D50}$), taustot (τ^*_{D50}), for (a) Albula 2016, (b) Navisence 2011, (c) Avançon 2019.

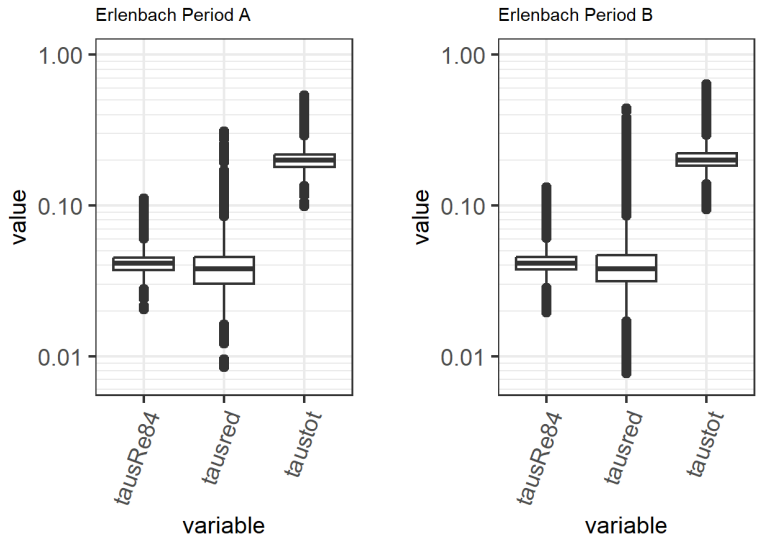

(d) (e)

Figure S31_contd. Boxplots of tausRe84 (τ^*_{Re84}), tausred ($\tau^{*'}_{D50}$), taustot (τ^*_{D50}), for (d) Erlenbach Period A, (e) Erlenbach Period B.